Molecular and Cellular Characterization of Imexon-resistant RPMI8226/I Myeloma Cells[1]

Katerina Dvorakova, Claire M. Payne, Margaret E. Tome, Margaret M. Briehl, Miguel A. Vasquez, Caroline N. Waltmire, Amy Coon, and Robert T. Dorr[2]

Arizona Cancer Center [K. D., M. A. V., C. N. W., A. C., R. T. D.] and Departments of Microbiology and Immunology [C. M. P.] and Pathology [M. E. T., M. M. B.], University of Arizona, Tucson, Arizona 85724

Abstract

Imexon is an aziridine-containing iminopyrrolidone with selective growth-inhibitory potency for multiple myeloma. Our previous research indicates that imexon induces mitochondrial alterations, oxidative stress, and apoptosis. This drug represents an interesting model drug with a nonmyelosuppressive profile to study the basic mechanisms leading to antitumor activity and resistance. The major purpose of this study was to characterize an imexon-resistant RPMI8226/I cell line that was developed from RPMI8226 cells by continuous exposure to imexon. No significant differences were observed in the sensitivity to several cytotoxic drugs, including mitoxantrone, mitomycin C, melphalan, methotrexate, cytarabine, cisplatin, vincristine, and paclitaxel, in the imexon-resistant cells. However, RPMI8226/I cells were cross-resistant to arsenic trioxide, doxorubicin, fluorouracil, etoposide, irinotecan, and especially IFN-α. The data from DNA microarray and Western blot analyses indicated that the levels of antiapoptotic proteins Bcl-2 and thioredoxin-2, which reside mainly in the mitochondria, are increased in RPMI8226/I cells. In addition, increased levels of lung resistance protein were detected in imexon-resistant cells. Expression of P-glycoprotein was not detected in RPMI8226/I cells. No loss of mitochondrial membrane potential or increase in the levels of reactive oxygen species was observed in RPMI8226/I cells after exposure to imexon; however, the levels of glutathione are increased in the RPMI8226/I cells. Transmission electron microscopy revealed significant changes in the mitochondrial morphology of RPMI8226/I cells, whereas no ultrastructural changes were observed in other cellular compartments. Imexon-resistant RPMI8226/I myeloma cells appear to have a unique mechanism of resistance that is associated with morphological alterations of mitochondria, increased protection against oxidative stress, elevated levels of glutathione, and enhanced expression of antiapoptotic mitochondrial proteins.

Introduction

Multiple myeloma is a uniformly fatal disease that is characterized by a clonal proliferation of neoplastic plasma cells in the bone marrow. At present, a cure for multiple myeloma has not been achieved with any chemotherapeutic regimen, and essentially all patients who respond initially to drug treatment will relapse and die of drug-resistant disease. Thus, the development of new anticancer agents with a nonmyelosuppressive profile that induce apoptosis seems to be an attractive perspective. Imexon is an aziridine-containing iminopyrrolidone that induces apoptosis with unique activity in multiple myeloma (Fig. 1; Refs. 1 and 2). This drug is currently synthesized for use in National Cancer Institute-sponsored clinical trials. Importantly, previous studies have shown that no myelosuppression was associated with imexon treatment in all species studied, including humans (3–5). In addition, imexon was active in myeloma cell lines overexpressing PGP[3] (6). In this regard, imexon may offer a unique opportunity for developing an agent that is nonmyelosuppressive and therapeutically active, as demonstrated in pilot Phase I solid tumor studies (3, 7, 8).

Recent mechanistic studies in human RPMI8226 myeloma cells have shown the effects of imexon on mitochondria (1, 9). Imexon induces oxidative stress, loss of mitochondrial membrane potential ($\Delta\psi_m$), the release of cytochrome *c* from mitochondria, ultrastructural alteration of the mitochondria, and, finally, apoptosis (1, 9). Significant mitochondrial swelling was one of the first changes detected as early as 4 h after imexon treatment in RPMI8226 cells (9). In addition, oxidized nucleotides were detected in the cytoplasm and possibly in the mitochondria of imexon-treated cells, but, surprisingly, they were not detected in the nucleus (1). We have also shown that mitochondrial DNA was affected by imexon treatment, whereas no damage was observed in nuclear DNA (9). Our previous data indicated that there is a high correlation in the different malignant cell lines between sensitivity to imexon, increased production of free radicals, and the loss of mitochondrial membrane potential (9). Moreover, significant reduction of imexon cytotoxic effects was induced when RPMI8226 myeloma cells were treated simultaneously

Received 8/22/01; revised 10/5/01; accepted 10/11/01.
[1] Supported by NIH Grants CA 23074 and 17094 (to R. T. D.) and National Cancer Institute Grant CA 71768 (to M. M. B.). K. D. and M. E. T. were partially supported by National Cancer Institute Grant CA 09213.
[2] To whom requests for reprints should be addressed, at Arizona Cancer Center, 1515 North Campbell Avenue, Tucson, AZ 85724. Phone: (520) 626-7892; Fax: (520) 626-2751; E-mail: bdorr@azcc.arizona.edu.

[3] The abbreviations used are: PGP, P-glycoprotein; GSH, glutathione; GSSG, glutathione disulfide; NEM, *N*-ethylmaleimide; MTT, 3-(4,5,-dimethylthiazol-2-yl)-2,5-diphenyltetrazolium bromide; HE, dihydroethidium; LRP, lung resistance protein; ROS, reactive oxygen species; topo, topoisomerase; Trx, thioredoxin; TRAF, tumor necrosis factor receptor-associated factor; PHGPx, phospholipid hydroperoxide glutathione peroxidase; MAPK, mitogen-activated protein kinase; TNF, tumor necrosis factor.

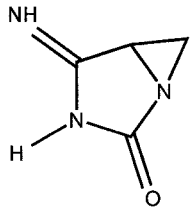

Fig. 1. Chemical structure of imexon.

with imexon and either thenoyltrifluoroacetone, an inhibitor of mitochondrial superoxide production, or *N*-acetyl-L-cysteine, which can act as an antioxidant or GSH precursor (1, 9). These data are consistent with mitochondrial oxidation and mitochondrial apoptotic signaling as mediators of the growth-inhibitory effects of imexon.

Imexon represents an interesting model drug to study the basic mechanisms leading to antitumor activity and resistance. Thus, we developed RPMI8226/I, a RPMI8226 myeloma cell line resistant to the growth-inhibitory effects of imexon to probe differences between the resistant cells and the parental cell line that might highlight mechanistic actions of the drug. In this report, we describe the characteristics of this cell line in terms of cancer drug cross-resistance patterns, the differential expression of the mitochondrial antiapoptotic proteins Bcl-2 and Trx-2, the susceptibility to the loss of mitochondrial membrane potential, and drug-induced production of ROS. In addition, DNA microarray analyses revealed differentially expressed genes in the imexon-resistant cells that may be important in maintaining the imexon-resistant phenotype.

Materials and Methods

Chemicals. Imexon (4-imino-1,3-diazabicyclo-[3.1.0]-hexanone), NEM, and arsenic trioxide were obtained from Sigma Chemical Co. (St. Louis, MO). MitoTracker Red (CMXRos) and HE (Hydroethidine) were purchased from Molecular Probes Inc. (Eugene, OR). Doxorubicin HCl was obtained from Fujisawa USA, Inc. (Deerfield, IL); paclitaxel (Taxol®), cisplatin (Platinol AQ), mitomycin C (Mutamycin), and etoposide phosphate (Etopophos) were obtained from Bristol-Myers Squibb Co. (Princeton, NJ); mitoxantrone (Novantrone) was obtained from Lederle Laboratories (Gosport, United Kingdom); vincristine sulfate was obtained from Eli Lilly and Co. (Indianapolis, IN); and IFN-α2b (Intron-A) was obtained from Schering-Plow (Kenilworth, NJ). The topoI inhibitor irinotecan (Camptosar) was obtained from Pharmacia Upjohn (Kalamazoo, MI). The alkylating agent melphalan HCl (98% purity) was obtained from Sigma Chemical Co. Three antimetabolites were tested, as supplied for commercial clinical use: (*a*) fluorouracil (5.9 μg/ml solution; American Pharmaceutical Partners, Los Angeles, CA); (*b*) cytarabine (Cetus Corp., Emeryville, CA); and (*c*) methotrexate (Immunex Corp., Seattle, WA). The stock solutions of drugs were prepared according to the manufacturers' instructions. The imexon stock solution (1 mg/ml) was prepared in PBS, filter-sterilized, and stored at −80°C. The arsenic trioxide stock solution (10 mg/ml) was prepared in 1 N NaOH. All other chemicals, unless noted otherwise, were of the highest purity available and were obtained from Sigma Chemical Co.

Cell Cultures and Viability Assays. The human myeloma RPMI8226 cell line was obtained from the American Type Culture Collection (Manassas, VA). RPMI8226/Dox40 and RPMI8226/MR20 cell lines were obtained from Dr. Alan List (University of Arizona). The imexon-resistant RPMI8266/I cell line was established in our laboratory by continuous exposure of RPMI8226 cells to increasing concentrations of imexon (up to a final concentration of 90 μM). RPMI8226/I cells were then maintained in 90 μM imexon for more than 6 months. All cell lines were cultured at 37°C in 5% CO_2 in RPMI 1640 (Life Technologies, Inc., Grand Island, NY) supplemented with 10% (v/v) heat-inactivated bovine calf serum (Hyclone Laboratories, Logan, UT), 2 mM L-glutamine, 100 units/ml penicillin, and 100 μg/ml streptomycin. Cellular dehydrogenase activity, which is considered to reflect mitochondrial activity and cell viability, was measured by a microculture MTT assay based on the ability of living cells to reduce MTT (Sigma Chemical Co.) to a blue formazan according to the method of Mosmann (10).

Transmission Electron Microscopy and Bright-Field Microscopy Studies. Transmission electron microscopy was used to detect morphological differences between RPMI8226 and RPMI8226/I cells. Cells (1×10^6) were fixed with 3% glutaraldehyde in 0.1 M cacodylate buffer (pH 7.2). The cells were then postfixed in 1% osmium tetroxide, dehydrated in a graded series of ethanols, and embedded in epoxy resin. Ultrathin sections were evaluated for morphological changes using a Philips CM12 transmission electron microscope (Eindhoven, the Netherlands).

For the quantitation of mitochondrial matrix granules, mitochondrial aggregates from 10 different RPMI8226 and RPMI8226/I cells were randomly photographed at a scope magnification of ×45,900. Prints were prepared, and the number and diameter of all matrix granules were measured (1 mm on print = 21.8 nm). The mean diameter (nm) ± SE was calculated for matrix granules in both cell lines. The statistical significance of the difference between mean values was determined at the 95% confidence level ($P < 0.05$) using Student's *t* test.

For bright-field microscopy studies, the RPMI8226 and RPMI8226/I cells were treated with imexon for 48 h. The cells were cytospun on slides using a Cytospin 2 centrifuge (Shandon, Pittsburgh, PA) and then fixed with 100% methanol for 2 min at room temperature, air-dried, and stained with DiffQuick stain (Life Technologies, Inc.).

GSH Analysis. Reverse-phase high-performance liquid chromatography was used to measure levels of GSH and GSSG. GSH and GSSG were extracted with perchloric acid and derivatized with iodoacetic acid and 1-fluoro-2,4-dinitrobenzene to form dinitrophenyl derivatives according to the protocol of Fariss and Reed (11). Chromatographic peaks were integrated using a PE NelsonTurboChrom 4 program (San Jose, CA). GSH and GSSG concentrations were normalized to total cellular protein measured as described previously (12).

Cytofluorometric Determination of $\Delta\psi_m$ and ROS. RPMI8226 and RPMI8226/I myeloma cell lines treated with various concentrations of imexon for 48 h were evaluated for changes in $\Delta\psi_m$ and ROS levels by staining with CMXRos and HE, as described previously (9). CMXRos is a lipophilic cationic dye that is accumulated in mitochondria with normal $\Delta\psi_m$. Briefly, the cells (0.5×10^6 cells/ml) were stained with 100 nM CMXRos for 30 min at 37°C, centrifuged, resuspended in 500 μl of PBS while kept on ice, and analyzed immediately on a flow cytometer (Becton Dickinson FACScan, San Jose, CA) using excitation at 488 nm and emission at 600 nm.

Oxidative damage was measured by staining with a nonfluorescent compound, HE, which is oxidized to the highly fluorescent ethidium by cellular oxidants (13). Cells (0.5×10^6 cells/ml) were stained at a final concentration of 2 μM HE for 30 min at 37°C, centrifuged, and resuspended in 500 μl of PBS while kept on ice. The cells were then analyzed by flow cytometry (excitation, 488 nm; emission, 620 nm).

Isolation of Mitochondrial and Cytosolic Fractions. Cytosolic and mitochondrial fractions were isolated from RPMI8226 and RPMI8226/I cells according to the method of Vander Heiden *et al.* (14). Briefly, the cells (200×10^6) were resuspended in 0.24 ml of ice-cold buffer A [20 mM HEPES, 10 mM KCl, 1.5 mM $MgCl_2$, 1 mM EDTA, 1 mM EGTA, 1 mM DTT, and 17 μg/ml phenylmethylsulfonyl fluoride (pH 7.4)]. Cells were incubated on ice, and after 30 min, sucrose solution (1 M) was added to achieve a final sucrose concentration of 250 mM. Cells were then homogenized immediately in a ground glass homogenizer (Kimble/Kontes, Vineland, NJ) and centrifuged for 10 min at $750 \times g$. The supernatant was then centrifuged at $10,000 \times g$ for 25 min. The resulting pellet representing the mitochondrial fraction was resuspended in buffer A containing 250 mM sucrose. The $10,000 \times g$ supernatant was then centrifuged at $100,000 \times g$ for 60 min to yield the cytosolic fraction in the supernatant. The protein concentrations were determined according to the method of Smith *et al.* (12).

Western Blot Analysis. Western blot analysis was performed as described previously (9). RPMI8226 and RPMI8226/I myeloma cells were lysed using lysis buffer [50 mM Tris (pH 8), 5 mM EDTA, 150 mM NaCl, and 0.5% NP40] supplemented with 1 mM phenylmethylsulfonyl fluoride, 1 μg/ml leupeptin, and 0.01 unit/ml aprotinin. Protein aliquots were loaded (10–20 μg/lane) on a 10–15% SDS-polyacrylamide gel for size fractionation by electrophoresis. The proteins were blotted onto Immobilon-P polyvinylidene difluoride transfer membrane (Millipore, Bedford, MA). The membranes were immunostained with either mouse anti-bcl-2 antibody (1:2,500; Santa Cruz Biotechnology, Santa Cruz, CA), mouse anti-cytochrome *c* monoclonal antibody (1:500; PharMingen, San Diego, CA), mouse anti-Trx-1 monoclonal antibody (1:5,000), or rabbit polyclonal anti-Trx-2 antibody (1:500). The anti-Trx-1 and anti-Trx-2 antibodies were kindly provided by Dr. Garth Powis (University of Arizona). The membranes were then incubated with goat antimouse or goat antirabbit IgG antibodies conjugated to horseradish peroxidase (1:40,000; Pierce, Rockford, IL). Antibody complexes were detected using the enhanced chemiluminescence detection system (ECL; Amersham Pharmacia Biotech, Piscataway, NJ). Finally, the membranes were stained for 5 min with Brilliant Blue G dye and destained with a 25% methanol:10% acetic acid solution to confirm equal protein loading in individual lanes (data not shown).

DNA Microarray. Total RNA was isolated from untreated RPMI8226 and RPMI8226/I cells (1×10^8) with Trizol reagent (Life Technologies, Inc.) according to the manufacturer's instructions. Poly(A)$^+$ RNA was isolated from total RNA using an Oligotex mRNA Midi Kit (Qiagen, Valencia, CA) according to the batch protocol. The final concentration of mRNA was adjusted to 0.5–1 μg/μl. mRNA (4 μg) was used to prepare cDNA probes labeled with Cy3 or Cy5. Briefly, 1 μg of oligo deoxythymidine (dT) was added to 11.4 μl of mRNA solution, and the mixture was heated at 70°C for 5 min and then placed on ice for 30 s. After incubation for 10 min at 25°C, 14.6 μl of Cy3 or Cy5 master mix were added (6 μl of 5× first-strand buffer, 3 μl of 0.1 M DTT, 3 μl of Cy3 or Cy5 dCTP, 0.6 μl of 25 mM each dATP, dGTP, dTTP, and 10 mM dCTP, and 2 μl of RNAsin (Life Technologies, Inc.). Then, 2 μl of Superscript reverse transcriptase (Life Technologies, Inc.) were added, and the mixture was incubated for 2 h at 42°C. The reaction was stopped by adding 2.65 μl of 25 mM EDTA. The RNA strands were degraded by adding 3.3 μl of 1 M NaOH. The solution was neutralized with 3.3 μl of 1 M HCl, and 5 μl of 1 M Tris (pH 6.8) were added. Unincorporated fluorescent nucleotides were removed using Centricon-30 microconcentrators (Millipore) and the QIAquick Nucleotide Removal Kit (Qiagen) according to the manufacturer's instructions. Purified, labeled cDNA probe was resuspended in 9 μl of water, 5 μl of 20× SSC, 2 μl of *Cot*1 DNA (10 mg/ml; Life Technologies, Inc.), and 4 μl of 1% SDS. Finally, the solution was boiled for 3 min, allowed to cool, and applied to the microarray under a coverslip. The slide was placed in a hybridization chamber and incubated for 14–18 h in a water bath at 64°C. After incubation, the slides were washed with 0.5× SSC and 0.01% SDS for 5 min, washed with 0.06× SSC and 0.01% SDS for 5 min, and washed twice with 0.06× SSC for 2 min. The slides were scanned with GSI Lumonics 5000 Scanner (Bedford, MA) using emission and absorption wavelength for Cy5 and Cy3.

We selected 550 genes from the first release of the UniGene library (Research Genetics, Huntsville, AL) based on their importance in cell cycle regulation, cancer, cell signaling, and apoptosis. *Escherichia coli* containing the vectors with the genes of interest were grown overnight, and PCR was performed on the culture using universal primers that work on each vector, according to the protocol provided by Research Genetics. An aliquot of each product was then verified on an agarose gel, and the remaining product was subsequently purified using a PCR purification kit (Clontech, Palo Alto, CA). The eluted DNA was lyophilized, resuspended in 20 μl of a solution containing 3× SSC and 0.1% Sarkosyl, and placed into 96-well plates in preparation for printing. DNA was spotted in duplicate onto DNA-Ready Type I slides (Clontech) using an Affymetrix GMS 417 Arrayer (Santa Clara, CA). After printing, the slides were allowed to dry and were placed in a desiccator until needed. Before hybridization, the DNA was cross-linked to the slides using a Strata-

linker (Stratagene) at 0.3 J, followed by a 1-min wash in 0.1% SDS and two 1-min washes in double-distilled water. The slides were allowed to dry completely at room temperature before hybridization.

Immnunohistochemical Analysis. For the evaluation of LRP and PGP expression in RPMI8226 and RPMI8226/I cells, a standard immunostaining assay with biotin-streptavidin-linked peroxidase detection method was used as described previously (15–17). Briefly, RPMI8226 and RPMI8226/I cells were cytospun on the slide, fixed with acetone, and immunostained with anti-LRP (1:800; kindly provided by Dr. R. Scheper; Department of Pathology, Free University Hospital, Amsterdam, the Netherlands) or anti-PGP (1:20; JSB-1; Accurate Chemical @ Scientific Corporation, Westbury, NY) monoclonal mouse antihuman antibody. The RPMI8226/Dox40 and RPMI8226/MR20 cell lines, which are known to express PGP and LRP, respectively, were used as a positive control. The secondary antibody was a biotinylated goat antimouse IgG antibody. The biotin was linked to streptavidin with bound peroxidase. The streptavidin-peroxidase complex was then allowed to react with diaminobenzidine and enhanced with copper sulfate.

Table 1 Cytotoxicity of different agents for RPMI8226 and RPMI8226/I myeloma cells

IC_{50} concentrations of different agents in RPMI8226 and RPMI8226/I human myeloma cells were determined using the MTT assay after 120 h of drug treatment. The results represent mean ± SD.

Drug	IC_{50}		Degree of resistance
	RPMI8226 cells	RPMI8226/I cells	
Imexon	20.6 ± 3.1 μM	119.6 ± 9.7 μM	5.8[a]
Mitoxantrone	0.118 ± 0.035 μM	0.121 ± 0.034 μM	1.03
Cisplatin	2.19 ± 0.26 μM	2.05 ± 0.3 μM	0.9
Arsenic trioxide	3.41 ± 0.58 μM	8.61 ± 0.98 μM	2.5[a]
NEM	26.4 ± 5.7 μM	42.1 ± 10.1 μM	1.6[a]
Taxol	0.81 ± 0.11 nM	0.89 ± 0.16 nM	1.1
IFN-α2	1,683 ± 176 units/ml	>100,000 units/ml	>60[a]
Vincristine sulfate	9.4 ± 0.4 nM	6.5 ± 0.4 nM	0.7
Doxorubicin	28.7 ± 4.6 nM	62.1 ± 8.6 nM	2.2[a]
Mitomycin C	0.10 ± 0.02 μM	0.06 ± 0.01 μM	0.6[a]
Cytarabine	0.74 ± 0.12 μM	1.05 ± 0.17 μM	1.4
5-Fluorouracil	0.83 ± 0.18 μM	3.48 ± 0.29 μM	4.2[a]
Methotrexate	0.042 ± 0.005 μM	0.042 ± 0.005 μM	1
Melphalan	8.3 ± 1.5 μM	17.7 ± 6.7 μM	2.1
Etoposide	0.049 ± 0.021 μM	0.232 ± 0.013 μM	4.7[a]
Irinotecan	0.89 ± 0.21 μM	2.54 ± 0.22 μM	2.9[a]

[a] Statistically significant difference between IC_{50} for RPMI8226 and RPMI8226/I cells ($P < 0.05$).

Results

Imexon-resistant RPMI8226/I Cell Line. Imexon-resistant RPMI8226/I myeloma cells were developed over a 6-month period by continuous stepwise exposure of RPMI8226 cells to escalating concentrations of imexon. Throughout this period, it was apparent that only increase in drug concentrations would be feasible because the cells were sensitive to small concentration changes and never exhibited tolerance to large increments of change in imexon concentration. The resultant drug-resistant RPMI8226/I cells grew in the presence of 90 μM imexon. The IC_{50} of imexon (as measured by MTT assay at 120 h) in the imexon-sensitive RPMI8226 cells was 20.6 μM, whereas that in RPMI8226/I cells was 119.6 μM. The difference in IC_{50} values indicates a 5.8-fold increase in IC_{50} for RPMI8226/I cells as compared with the parental cell line. This resistance appears to be stable because the IC_{50} of imexon for RPMI8226/I cells grown without imexon for 4 months was 131 μM.

Cross-Resistance Pattern of RPMI8226/I Cells. The RPMI8226/I cells were evaluated for cross-resistance to several classical anticancer drugs. No significant differences in the IC_{50} values were found for most DNA-interacting drugs, including mitomycin C, melphalan, mitoxantrone, and cisplatin, or for the mitosis-blocking drugs paclitaxel and vincristine sulfate (Table 1). The RPMI8226/I cells were cross-resistant to the cytotoxic effects of the topoI inhibitor irinotecan, the topoII inhibitor etoposide, the antimetabolite fluorouracil, the anthracycline doxorubicin, and especially IFN-α2b (IFN-α), which is sometimes used in the treatment of multiple myeloma (18–20). The IC_{50} values of IFN-α at 120 h were 1,683 and >100,000 units/ml, respectively, for RPMI8226 and RPMI8226/I cells.

Arsenic trioxide (As_2O_3) and NEM are toxic to RPMI8226 cells. However, we found that RPMI8226/I cells are partially protected against the effects of these compounds. The IC_{50} at 120 h of As_2O_3 in RPMI8226 cells and RPMI8226/I cells was 3.41 and 8.61 μM, respectively. The IC_{50} at 120 h of NEM in RPMI8226 cells and RPMI8226/I cells was 26.4 and 42.1 μM, respectively.

GSH and GSSG Levels in RPMI8226 and RPMI8226/I Cells. Because previous studies have shown that imexon induces oxidative stress and depletion of GSH, we tested whether imexon resistance is associated with an increase in GSH concentrations. In RPMI8226 cells, the GSH concentration was 92.1 ± 8.5 nmol/mg protein; however, in RPMI8226/I cells, GSH levels were 147.0 ± 7.2 nmol/mg protein ($P < 0.05$). This change represents a 60% increase in GSH levels. Similarly, GSSG concentrations were increased from 1.43 ± 0.14 nmol/mg protein in RPMI8226 cells to 2.79 ± 0.35 nmol/mg protein in RPMI8226/I cells ($P < 0.05$). The GSH:GSSG ratio was 64.4 in RPMI8226 cells and 52.8 in RPMI8226/I cells. This indicates a slight increase in oxidized GSH.

Oxidative Stress and Disruption of Mitochondrial Membrane Potential ($\Delta\psi_m$) after Imexon Treatment. Imexon treatment of the imexon-sensitive RPMI8226 cells is known to cause both increased ROS formation and loss of $\Delta\Psi_m$ (9). To test whether the imexon-resistant RPMI8226/I cells show a similar response, we monitored ROS and $\Delta\Psi_m$ in both cell lines after a 48-h treatment with various concentrations of imexon (Fig. 2). As seen previously, the RPMI8226 cells displayed a dose-dependent loss of $\Delta\Psi_m$ and an increase in the levels of ROS. In contrast, less significant changes in $\Delta\Psi_m$ and no increase in ROS levels were observed in RPMI8226/I cells after treatment with up to 270 μM imexon (Fig. 2, *A* and *B*). After treatment with 180 μM imexon for 48 h, 84% of imexon-sensitive cells lost $\Delta\Psi_m$ compared with only 25% of the imexon-resistant cells ($P < 0.05$).

Expression of Bcl-2, Trx-1, and Trx-2 in RPMI8226 Cells and RPMI8226/I Cells. Bcl-2 is known to protect cells against apoptosis and oxidative stress and is localized

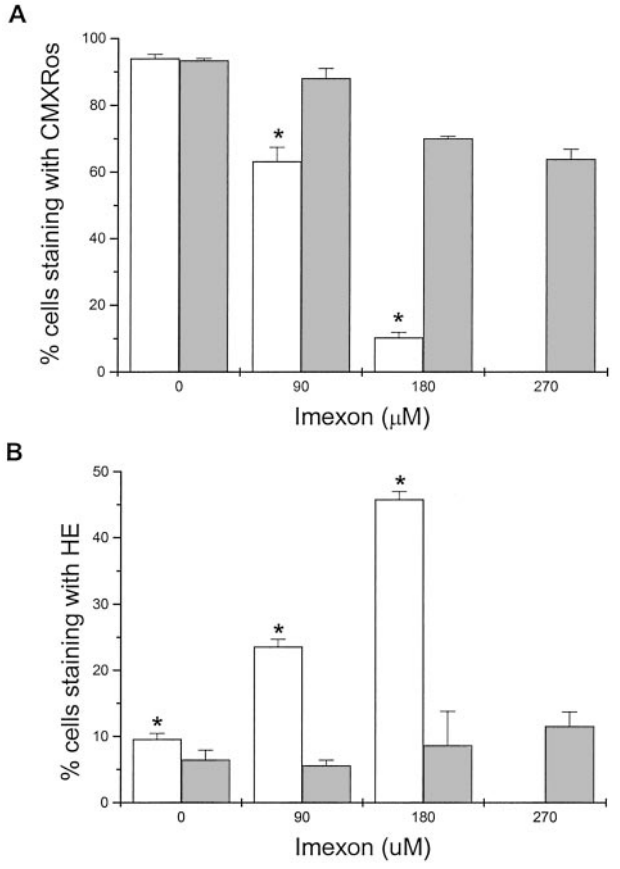

Fig. 2. Changes in $\Delta\Psi_m$ and ROS in RPMI8226 and RPMI8226/I cells after imexon treatment measured by flow cytometry. Imexon-sensitive (RPMI8226) and imexon-resistant (RPMI8226/I) myeloma cells were treated for 48 h with various concentrations of imexon and stained with CMXRos or HE to detect changes in $\Delta\Psi_m$ and ROS, respectively. *A* represents the percentage of RPMI8226 cells (□) and RPMI8226/I cells (■) that accumulate the mitochondrial dye CMXRos, indicating high $\Delta\Psi_m$. The percentage of RPMI8226 cells (□) and RPMI8226/I cells (■) producing ROS is indicated by the enhanced fluorescence of the oxidized form of HE (*B*). Imexon-sensitive RPMI8226 myeloma cells were not tested at 270 μM imexon because the cells do not survive this treatment for 48 h. Data represent the mean ± SE of three experiments. The *asterisks* indicate significant difference compared with the imexon-resistant cell line ($P < 0.05$).

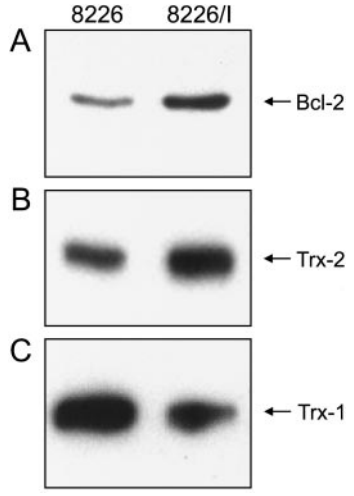

Fig. 3. Expression of Trx-1, Trx-2, and Bcl-2 in RPMI8226 and RPMI8226/I cells. Immunoblots of Bcl-2 (*A*), Trx-2 (*B*), and Trx-1 (*C*) in RPMI8226 cells and RPMI8226/I cells.

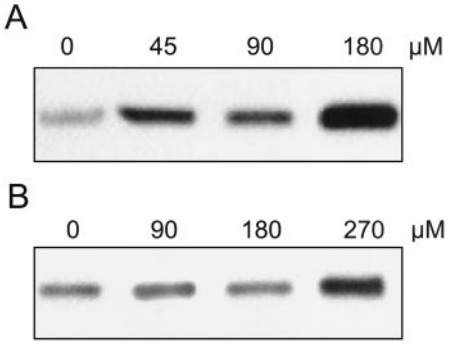

Fig. 4. Imexon-induced cytochrome *c* release from the mitochondria into the cytosol. Immunoblots of cytosolic cytochrome *c* (*A*) after 48 h of imexon treatment are shown in the control RPMI8226 cells treated with 0, 45, 90, and 180 μM imexon. *B* represents immunoblots of cytosolic cytochrome *c* in imexon-resistant RPMI8226/I cells treated for 48 h with 0, 90, 180, and 270 μM imexon.

mainly in the mitochondria. Therefore, the expression of Bcl-2 was measured by Western blot analysis, and increased levels were detected in the RPMI8226/I cells (Fig. 3*A*). Trx-2 is also localized in the mitochondria, and the expression of this antioxidant protein is associated with protection against apoptosis (21). We evaluated whether levels of Trx-2 are similarly increased in the RPMI8226/I cells. The data show that levels of Trx-2 are higher in imexon-resistant cells than in RPMI8226 cells (Fig. 3*B*). Interestingly, in RPMI8226/I cells, the levels of another member of the Trx family, cytosolic Trx-1, were decreased (Fig. 3*C*).

Inhibition of Cytochrome *c* Release from RPMI8226/I Cells. The release of cytochrome *c* from the outer surface of the inner mitochondrial membrane is one of the early steps of apoptosis and results in the activation of the apoptotic cascade. We have previously shown that imexon induces a time-dependent release of cytochrome *c* into the cytosol in imexon-sensitive RPMI8226 myeloma cells (9). Therefore, we compared cytochrome *c* release from the mitochondria of RPMI8226 *versus* RPMI8226/I cells after treatment with various concentrations of imexon for 48 h. A dose-dependent release of cytochrome *c* from the mitochondria was observed in imexon-treated RPMI8226 cells (Fig. 4*A*). However, a significantly higher concentration of imexon was necessary to induce this effect in the imexon-resistant cells. The release of cytochrome *c* was not detected in the imexon-resistant cells until the concentration of imexon reached 270 μM (Fig. 4*B*).

Morphological Alterations in RPMI8226/I Cells. Transmission electron microscopy was used to evaluate ultrastructural differences between RPMI8226 cells and RPMI 8226/I cells. The only apparent difference detected between the two cell lines involved mitochondrial ultrastructure (Fig. 5). In the imexon-resistant RPMI8226/I cells, the number of cristae

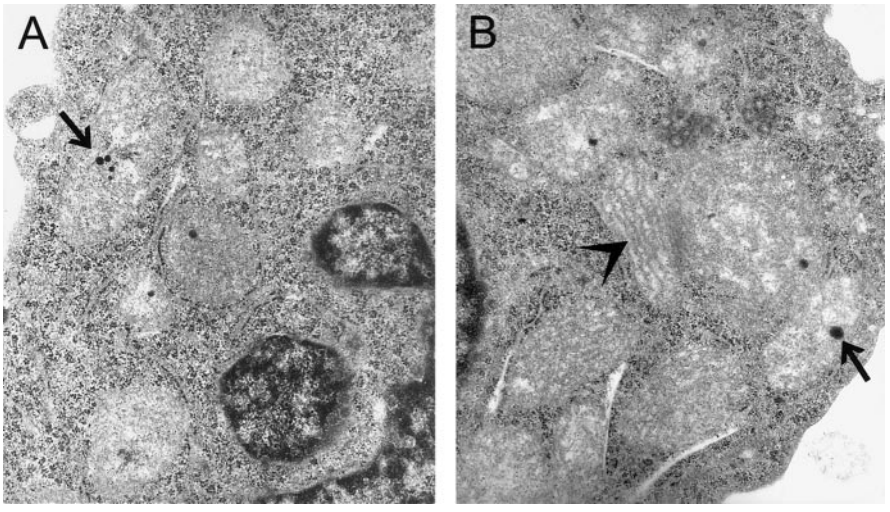

Fig. 5. Electron microscopy of RPMI8226 and RPMI8226/I cells. *A* and *B* represent typical electron micrographs of imexon-sensitive RPMI8226 (*A*) and imexon-resistant RPMI8226/I cells (*B*). Note the increase in cristae in imexon-resistant cells (*B, arrowhead*), giving the mitochondria a more electron-dense appearance. The matrix granules (calcific bodies) are larger in imexon-resistant cells (*B, arrow*) compared with imexon-sensitive cells (*A, arrow*).

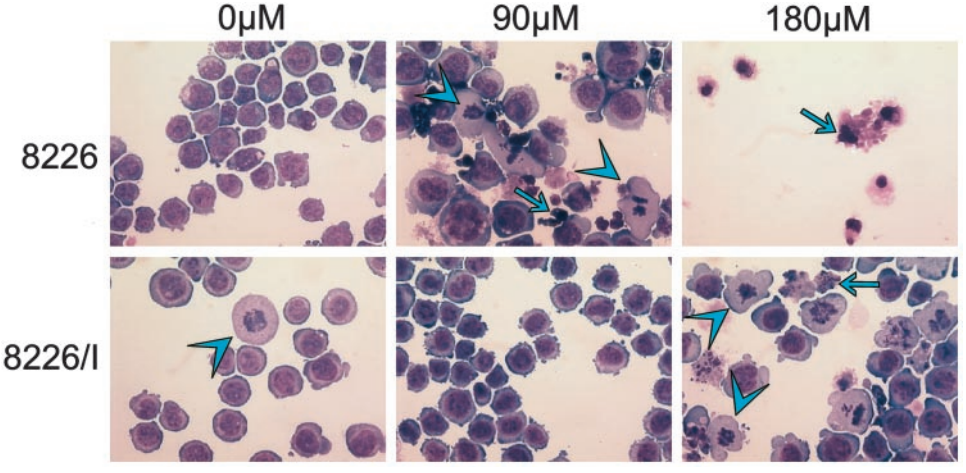

Fig. 6. Bright-field microscopy of RPMI8226 and RPMI8226/I cells treated with imexon. Images of RPMI8226 and RPMI8226/I cells treated with 0, 90, and 180 μM imexon for 48 h are shown. *Arrows* indicate apoptotic cells; *arrowheads* indicate cells undergoing mitosis.

was dramatically increased. These cristae were spaced close together and arranged parallel to the longitudinal axis of the mitochondria (Fig. 5*B*). In addition, the mean diameter (88.5 $\pm$ 4.0 nm) of the intramitochondrial matrix granules from the RPMI 8226/I cells (Fig. 5*B*) was significantly greater than that of the intramitochondrial matrix granules of the RPMI 8226 cells (60.1 $\pm$ 3.6 nm; $P < 0.05$; Fig. 5*A*). The frequency of the matrix granules was also compared. About one-third (28.8 $\pm$ 5.1%) of the mitochondria from the RPMI 8226/I cells contained matrix granules as compared with 24.2 $\pm$ 7.2% of the RPMI 8226 cells; however, this difference was not statistically significant ($P > 0.05$).

Apoptosis and mitotic arrest induced by 48-h imexon treatment in RPMI8226 and RPMI8226/I cells are displayed in Fig. 6. As expected, RPMI8226/I cells were unaffected by treatment with 90 μM imexon. In contrast, we found typical features of apoptosis in RPMI8226 cells treated with 90 μM imexon (Fig. 6). At this treatment level, we also observed a fraction of RPMI8226 cells in mitotic arrest (Fig. 6). Morphological evaluation revealed that the RPMI8226 cells treated with 180 μM imexon for 48 h were mostly apoptotic. In contrast, we found normal cells, apoptotic cells, and a large fraction of mitotic cells in the RPMI8226/I cells treated with 180 μM imexon (Fig. 6).

Immunohistochemical Analysis of PGP and LRP Expression. Immunohistochemical analysis for LRP and PGP revealed that RPMI8226/I cells have a higher expression level of LRP than RPMI8226 cells, whereas no alteration in expression of PGP was detected in RPMI8226/I cells (Fig. 7). As a positive control for PGP and LRP expression, RPMI8226/Dox40 cells and RPMI8226/MR20 cells were used, respectively (22, 23).

DNA Microarray. DNA microarray hybridization was used to evaluate the changes in gene expression due to the development of imexon resistance. The method of detailed analysis of data is available online.[4] Four different experiments were performed. According to our selection criteria, the expression of a gene was considered altered if: (*a*) the change was consistent in three experiments; and (*b*) there

[4] http://microarray.azcc.arizona.edu/aboutFiles/about.shtml.

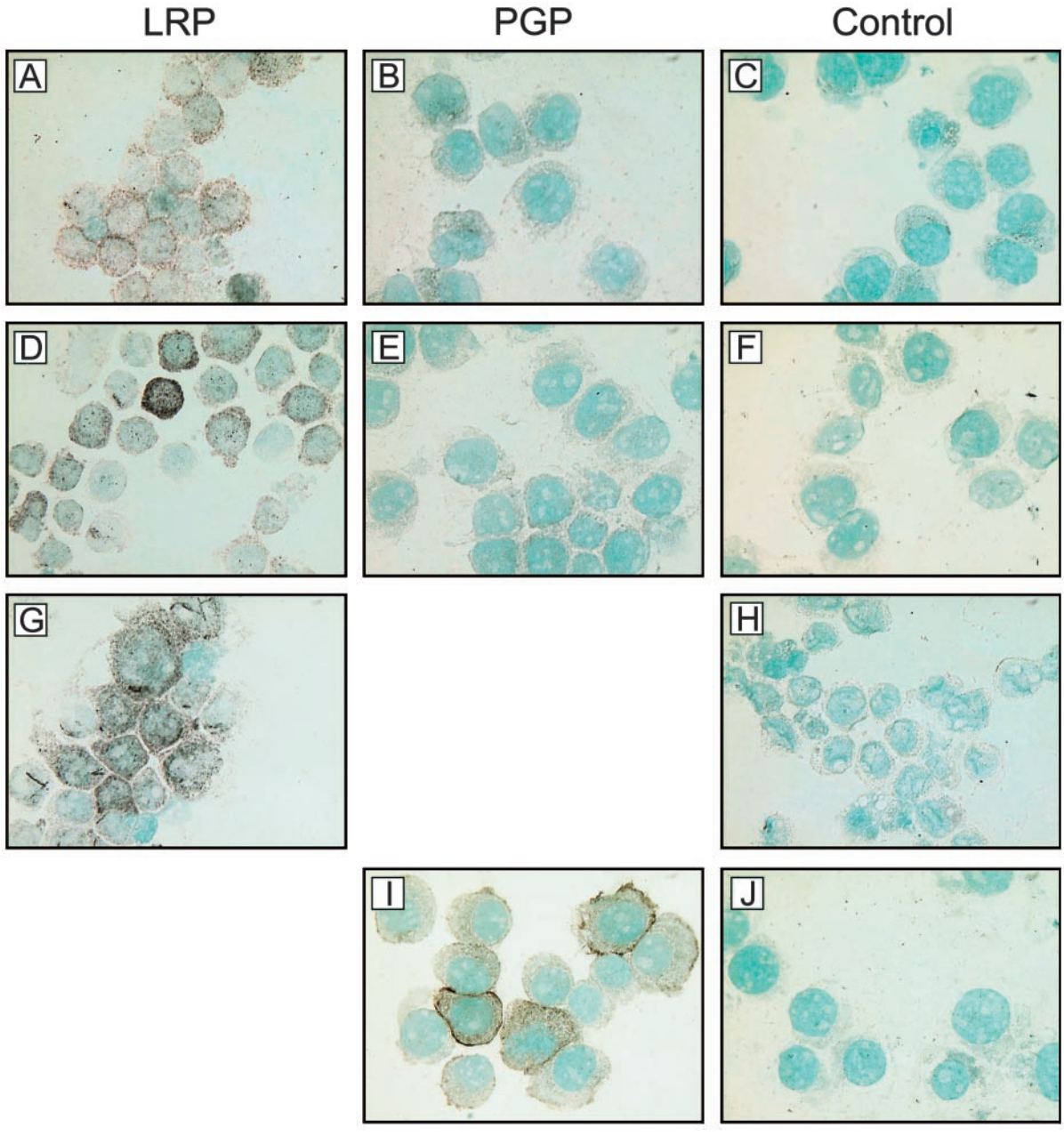

Fig. 7. Expression of LRP and PGP in RPMI8226 and RPMI8226/I cells. The slides were immunostained with monoclonal antibody against LRP (*A, D,* and *G*) and with monoclonal antibody against PGP (*B, E,* and *I*). The unstained cells (negative controls) are also displayed (*C, F, H,* and *J*). *A–C* represent RPMI8226 cells, *D–F* represent RPMI8226/I cells, *G* and *H* represent RPMI8226/MR20 cells (LRP-positive cells), and *I* and *J* represent RPMI8226/Dox40 cells (PGP-positive cells).

was a difference of at least of 1 SD in expression for two or more experiments. Observations in which the fluorescent signals were <140% of the background intensities were excluded. The median of the mean of the expression ratio for differentially expressed genes was calculated and is given in Table 2. We found the up-regulation of genes with known roles in protection against oxidative stress and apoptosis, including mitochondrial *Trx*, *bcl-2*, *TRAF1*, and *PHGPx*, in RPMI8226/I cells. Except for TRAF1, these proteins are localized mostly within mitochondria. The heat shock protein 90-related protein, TRAP1, and Noxa are other mitochondrial proteins that are overexpressed in imexon-resistant cells (24, 25). Other genes that were found to be up-regulated in RPMI8226/I cells included genes coding for ribosomal proteins, proteins involved in cell signaling, and proteins involved in regulation of the cell cycle, such as *jun D*, *v-myc homologue*, *CD27L*, *MAPK 1*, *MAPK kinase kinase 5*, *Rb-binding proteins*, and *cyclin G1*. Interestingly, we also found elevated expression of *major vault protein/LRP* mRNA in imexon-resistant cells. The expression of mRNA for two cy-

Table 2 DNA microarray in RPMI8226 and RPMI8226/I myeloma cells

This list indicates the proteins for which the mRNA was up-regulated (A) or down-regulated (B) consistently in three experiments, and the difference of at least 1 SD in expression was observed in two or more separate experiments. Each experiment consisted of duplicate samples. The numbers indicate median expression factor in three or more experiments.

A. Proteins for which mRNA was up-regulated

Increased expression of mRNA in RPMI8226/I cells	Median expression ratio
CD36 antigen (collagen type I receptor)[a]	34.51
PHGPx[a]	33.75
TNF (ligand) superfamily member 7(CD27L)[a]	19.06
CDC28 protein kinase[a]	18.64
Neutral sphingomyelinase[a]	18.62
HnRNP methyltransferase[a,b]	2.93
Arachidonate 12-lipoxygenase[a]	2.39
Ribosomal protein L10a[a]	2.15
Phorbol-12-myristate-13-acetate-induced protein (Noxa)[a]	2.15
Hydroxyacyl glutathione hydrolase	2.04
Cyclin G1[a]	1.96
Cyclin-dependent kinase 4	1.90
High-mobility group (nonhistone chromosomal protein)	1.86
MAPKK 1 (MEK1)[a]	1.83
TRAF1	1.82
Retinoblastoma-binding protein 4	1.81
Major vault protein	1.77
Eukaryotic translation initiation factor 3	1.73
E2F transcription factor 4	1.73
S-adenosylhomocysteine hydrolase	1.73
Heat shock protein 75 (TRAP1)	1.72
Methionine aminopeptidase	1.69
Ribosomal protein L32	1.65
AML1 oncogene	1.65
Trx (mitochondrial)	1.64
Bcl-2[a]	1.63
Heat shock protein 10 kD	1.62
Ribosomal protein L31[a]	1.60
v-myc oncogene avian myelocytomatosis viral homologue[a]	1.59
Jun D proto-oncogene	1.54
Phosphoinositide-3-kinase	1.51
ERG1-binding protein 2[a]	1.50
Ribosomal protein S5[a]	1.49
Macropain	1.48
Intercellular adhesion molecule 3	1.43
Cytochrome P450,51[a]	1.42
P450 (cytochrome) oxidoreductase[a]	1.34
Nuclear matrix protein p84[a]	1.28

B. Proteins for which mRNA was down-regulated

Decreased expression of mRNA in RPMI8226/I cells	Median expression ratio
Fibronectin[a]	0.1
GSH *S*-transferase M2[a]	0.11
Glutathione peroxidase 1[a]	0.41
GLUT5[a]	0.44
MutL homologue 1	0.66
Step II splicing factor SLU 7	0.76
Myeloid cell nuclear differentiation antigen[a]	0.82
Transferrin receptor (p90)	0.84

[a] Difference of 2 SDs in one or more experiments.
[b] HnRNP, heterogenous nuclear ribonuclear protein; MAPKK 1, MAPK Kinase 1; MEK, mitogen-activated protein/extracellular signal-regulated kinase.

tosolic proteins that may play a role in the protection against ROS, *GSH S-transferase M2* and *GSH peroxidase 1*, was down-regulated in RPMI8226/I cells.

Discussion

The major aim of this study was to characterize the imexon-resistant RPMI8226/I cell line. To accomplish this, the RPMI8226/I myeloma cell line was developed with stable resistance to the growth-inhibitory effects of imexon. No cross-resistance was observed to several classical anticancer drugs including mitomycin C, melphalan, cytarabine, methotrexate, paclitaxel, vincristine, cisplatin, and mitoxantrone. These data, together with our previous reports, suggest that imexon does not directly target DNA and that its mechanism of action is distinct from that of natural products such as paclitaxel or vincristine (1, 9). In addition, previous studies have shown that imexon is active in myeloma cell lines overexpressing PGP (6). Thus, we speculate that the mechanism of resistance to imexon is different from that of existing cytotoxic anticancer drugs that target DNA or microtubules. This is supported by our finding that PGP expression is not elevated in RPMI8226/I cells, whereas expression of LRP, the protein associated with vault expression in multidrug-resistant cells, is higher in RPMI8226/I cells (15, 26).

Other oxidizing agents appear to act similarly to imexon. For example, NEM depletes thiols by binding to the sulfhydryl group of cysteine. It was reported that NEM affected rat liver mitochondria by opening the mitochondrial permeability transition pore (27). This effect could be completely blocked with DTT or β-mercaptoethanol (27). Similarly, imexon cytotoxicity can be antagonized by *N*-acetylcysteine (1). The partial cross-resistance of RPMI8226/I myeloma cells to the effects of NEM suggests that sensitivity to thiol depletion is decreased in RPMI8226/I cells compared with the parental RPMI8226 cells. This phenomenon could be explained by our subsequent finding that RPMI8226/I cells have higher concentrations of GSH than the parental cell line.

RPMI8226/I cells are also cross-resistant to the cytotoxic effects of As_2O_3. Whereas the precise mechanism of As_2O_3 toxicity is not completely understood, it is believed to involve mitochondrial alteration and binding to the sulfhydryl group of cysteine residues. In this regard, the pattern of imexon effects is similar to the mechanistic effects of arsenic trioxide. For example, both imexon and arsenic trioxide induce (*a*) apoptosis, (*b*) loss of mitochondrial membrane potential, (*c*) depletion of GSH, (*d*) formation of ROS, and (*e*) release of cytochrome *c* into the cytosol (28–34). Several studies also suggest that arsenic compounds may act on mitochondria to induce apoptosis via a direct effect on the mitochondrial permeability transition pore (34, 35). Furthermore, Bcl-2 expression induced by gene transfer prevented all hallmarks of arsenite-induced cell death (34). Similarly, we have also shown that cells transfected with bcl-2 are protected against imexon-induced cytotoxicity (1). As with imexon, antioxidants antagonize As_2O_3-induced cytotoxicity, and GSH depletion by buthionine sulfoximine enhances As_2O_3-induced apoptosis (29, 36). More recent mechanistic studies have revealed that arsenite binds to the sulfhydryl groups of tu-

bulin, and this leads to the induction of mitotic arrest and apoptosis (37–39). Interestingly, our studies also indicate that imexon induces mitotic arrest in both imexon-sensitive and imexon-resistant cells.

Arsenic trioxide at low doses has been shown to induce clinical remissions in patients with acute promyelocytic leukemia without severe toxicity (40, 41). This compound is now being extensively studied as an effective drug for the treatment of acute promyelocytic leukemia and possibly other leukemias. The recent study of Rousselot *et al.* (42) demonstrated that arsenic trioxide can inhibit the viability and growth of plasmacytoma cell lines and freshly isolated plasma cells from myeloma patients. Importantly, no significant bone marrow suppression associated with As_2O_3 treatment was observed in *in vivo* studies (40, 43). A similar lack of myelosuppression was reported after treatment with imexon (3). These similarities in the mechanisms of action of As_2O_3 and imexon, together with the cross-resistance of imexon-resistant cells to As_2O_3, suggest that these two drugs may have a similar mode of action. Imexon may thus represent a new class of drugs that is active and lacks the toxicity of As_2O_3.

The imexon-resistant myeloma cells were not cross-resistant to DNA cross-linking drugs (mitomycin C and melphalan) but did exhibit some resistance to topoI and topoII inhibitors (irinotecan and etoposide, respectively) and to fluorouracil and doxorubicin. Some of these effects are probably due to the overexpression of the LRP (major vault protein) multidrug resistance protein in RPMI8226/I cells. However, for all drugs except IFN-α, the degree of cross-resistance was lower than that to the inducing drug, imexon. In contrast, the RPMI8226/I cells are much more resistant to IFN-α than to imexon. One of the effects of IFNs is cell growth-inhibitory activity, possibly mediated by a marked down-regulation of new protein synthesis (44, 45). However, the mechanism behind this inhibition is not fully understood. Perhaps the imexon-resistant cells have alterations in the cell signaling pathways affected by IFN-α, resulting in the reduced sensitivity to IFN-α. Currently, studies are being performed in our laboratory to evaluate the resistance of RPMI8226/I cells to IFN-α.

Previously, we have reported that sensitivity to the cytotoxic effects of imexon correlates with a loss of $\Delta\psi_m$ and increased concentrations of ROS (9). Here we have shown that normal $\Delta\psi_m$ and low levels of ROS are maintained after imexon treatment in RPMI8226/I cells. In contrast, there is a dose-dependent increase in ROS and loss of $\Delta\psi_m$ in RPMI8226 cells treated with imexon. These results suggest that oxidative stress plays a significant role in the mechanism of imexon action.

Cytochrome *c* release from the mitochondria is associated with the initiation of the apoptotic cascade. Its release is known to result in the activation of several caspases, including caspase-9 followed by caspase-3. In RPMI8226/I cells, the release of cytochrome *c* was observed only at high concentrations of imexon, indicating the inhibition of apoptosis in these cells at mitochondria.

Because imexon induces apoptosis, oxidative stress, and mitochondrial alterations, we speculated that expression of antiapoptotic and antioxidant proteins would be increased in imexon-resistant RPMI8226/I myeloma cells. The Western blot analyses have shown that RPMI8226/I cells have significantly elevated levels of Bcl-2 (Fig. 3*A*). Overexpression of another mitochondrial antioxidant protein, Trx-2, in RPMI8226/I cells was also found by Western blot analysis (Fig. 3*B*). Bcl-2 and Trxs have been shown to play an important role in the protection against apoptosis, and they alter the cellular response to oxidative stress (46–49). Moreover, recent studies suggest that Trx-2 is more resistant to oxidation than cytosolic Trx-1 (50). This, together with the finding that imexon-resistant cells have a lower GSH:GSSG ratio, indicating significant oxidative stress, may partially explain the reduced levels of Trx-1 in RPMI8226/I cells.

The intramitochondrial matrix granules from the RPMI8226/I cells had a greater diameter compared with those from the imexon-sensitive cells. This may indicate a bcl-2-mediated response to increased calcium levels within the cytosol of the RPMI8226/I cells. The RPMI8226/I cells also exhibited an increased number of cristae, an ultrastructural finding associated with an energized state of mitochondria, perhaps in response to an increased energy demand by the cell. Thus, increased mitochondrial function and storage of Ca^{2+} may be responsible, in part, for the resistance phenotype.

The increased levels of Bcl-2 and Trx-2, together with the observation that high concentrations of imexon are necessary to release the cytochrome *c* from mitochondria of imexon-resistant cells, suggest that mitochondria of RPMI8226/I cells may be biochemically different from those in the imexon-sensitive myeloma cells. In agreement with Western blot data, in RPMI8226/I cells, the expression of bcl-2 and mitochondrial Trx mRNA is increased. The DNA microarray data also showed that the expression of PHGPx, an enzyme involved in the protection against oxidative stress, is significantly increased in imexon-resistant cells. PHGPx appears to be a good candidate for further mechanistic study because the long form of PHGPx, which resides in the mitochondrial membrane, has been shown to inhibit apoptosis by inhibiting peroxidation of cardiolipin. Unoxidized cardiolipin binds cytochrome *c* and thereby prevents cytochrome *c* release from mitochondria (51). However, it should be noted that the differential gene analyses were performed on cells harvested shortly after imexon treatment and may therefore include genes involved in the acute response or repair of imexon-induced cellular injury. Additional studies are planned to evaluate the time course of gene expression after imexon treatment.

In RPMI8226/I cells, we also found increased expression of mRNA coding for proteins involved in cell signaling and regulation of the cell cycle, such as jun D, v-myc homologue, TRAF1, and CD27L. Interestingly, CD27L binds CD27, a member of the subfamily of TNF receptors (TNF receptor II) that do not have a death domain and promote cell survival instead of apoptosis (52). Moreover, the increased mRNA expression of another protein involved in this survival pathway, TRAF1, was observed in RPMI8226/I cells. TRAF proteins are recruited to TNF receptor II after ligand binding and

can then initiate the activation of MAPK/extracellular signal-regulated kinase cascades that leads to cell survival (52).

Immunohistochemical analysis also confirmed microarray data indicating increased expression of LRP in RPMI8226/I cells. LRP plays a role in multidrug resistance, and its expression is associated with poor prognosis; however, its precise mechanism in mediating chemotherapy resistance is unknown (26, 53).

Overall, these results suggest that chronic exposure of myeloma cells to imexon induces increased expression of antioxidant and antiapoptotic proteins, especially those found in mitochondria. Combined with oxidative changes and the marked swelling of mitochondria after imexon treatment in drug-sensitive myeloma cells, this pattern suggests that imexon may target mitochondria, leading to oxidation and resultant apoptosis.

Acknowledgments

We are grateful Dr. Ray Nagle and Yvette Frutiger (Department of Pathology, The University of Arizona) for assistance with immunostaining.

References

1. Dvorakova, K., Payne, C. M., Tome, M. E., Briehl, M. M., McClure, T., and Dorr, R. T. Induction of oxidative stress and apoptosis in myeloma cells by the aziridine-containing agent imexon. Biochem. Pharmacol., *60:* 749–758, 2000.
2. Salmon, S. E., and Hersh, E. M. Sensitivity of multiple myeloma to imexon in the human tumor cloning assay. J. Natl. Cancer Inst. (Bethesda), *86:* 228–230, 1994.
3. Micksche, M., Colot, M., Uchida, A., Kokoschka, E. M., Luger, T. A., Dittrich, C., Moser, K., Rainer, H., Lenzhofer, R., Kolb, R., Jakesz, R., Schempeir, M., Kokron, O., Zwick, H., Scheiner, A., Flicker, H., and Sagaster, P. Immunomodulation in cancer patients by synthetic biological response modifiers. Cancer Treatment Symposia, *1:* 27–35, 1985.
4. Dorr, R. T., Liddil, J. D., Klein, M. K., and Hersh, E. M. Preclinical pharmacokinetics and antitumor activity of imexon. Investig. New Drugs, *13:* 113–116, 1995.
5. Bicker, U. F. BM06 002: a new immunostimulating compound. *In:* M. A. Chirigos (ed.), Immune Modulation and Control of Neoplasia by Adjuvant Therapy, pp. 389–401. New York: Raven Press, 1978.
6. Hersh, E. M., Gschwind, C. R., Taylor, C. W., Dorr, R. T., Taetle, R., and Salmon, S. E. Antiproliferative and antitumor activity of the 2-cyanoaziridine compound imexon on tumor cell lines and fresh tumor cells *in vitro*. J. Natl. Cancer Inst. (Bethesda), *84:* 1238–1244, 1992.
7. Sagaster, P., Kokoschka, E. M., Kokron, O., and Micksche, M. Antitumor activity of imexon. J. Natl. Cancer Inst. (Bethesda), *87:* 935–936, 1995.
8. Micksche, M., Kokoschka, E. M., Sagaster, P., and Bicker, U. Phase I study for a new immunomodulating drug, BM 06 002, in man. *In:* M. A. Chirigos (ed.), Immune Modulation and Control of Neoplasia by Adjuvant Therapy, pp. 403–413. New York: Raven Press, 1978.
9. Dvorakova, K., Waltmire, C. N., Payne, C. M., Tome, M. E., Briehl, M. M., and Dorr, R. T. Induction of mitochondrial changes in myeloma cells by imexon. Blood, *97:* 3544–3551, 2001.
10. Mosmann, T. Rapid colorimetric assay for cellular growth and survival: application to proliferation and cytotoxicity assays. J. Immunol. Methods, *65:* 55–63, 1983.
11. Fariss, M. W., and Reed, D. J. High-performance liquid chromatography of thiols and disulfides: dinitrophenol derivatives. Methods Enzymol., *143:* 101–109, 1987.
12. Smith, P. K., Krohn, R. I., Hermanson, G. T., Mallia, A. K., Gartner, F. H., Provenzano, M. D., Fujimoto, E. K., Goeke, N. M., Olson, B. J., and Klenk, D. C. Measurement of protein using bicinchoninic acid [published erratum appears in Anal. Biochem., *163:* 279, 1987]. Anal. Biochem., *150:* 76–85, 1985.
13. Rothe, G., and Valet, G. Flow cytometric analysis of respiratory burst activity in phagocytes with hydroethidine and 2′,7′-dichlorofluorescin. J. Leukocyte Biol., *47:* 440–448, 1990.
14. Vander Heiden, M. G., Chandel, N. S., Williamson, E. K., Schumacker, P. T., and Thompson, C. B. Bcl-x_L regulates the membrane potential and volume homeostasis of mitochondria. Cell, *91:* 627–637, 1997.
15. Scheper, R. J., Broxterman, H. J., Scheffer, G. L., Kaaijk, P., Dalton, W. S., van Heijningen, T. H., van Kalken, C. K., Slovak, M. L., de Vries, E. G., van der Valk, P., *et al.* Overexpression of a M_r 110,000 vesicular protein in non-P-glycoprotein-mediated multidrug resistance. Cancer Res., *53:* 1475–1479, 1993.
16. List, A. F., Spier, C. M., Cline, A., Doll, D. C., Garewal, H., Morgan, R., and Sandberg, A. A. Expression of the multidrug resistance gene product (P-glycoprotein) in myelodysplasia is associated with a stem cell phenotype. Br. J. Haematol., *78:* 28–34, 1991.
17. Grogan, T., Dalton, W., Rybski, J., Spier, C., Meltzer, P., Richter, L., Gleason, M., Pindur, J., Cline, A., Scheper, R., *et al.* Optimization of immunocytochemical P-glycoprotein assessment in multidrug-resistant plasma cell myeloma using three antibodies. Lab. Investig., *63:* 815–824, 1990.
18. Huang, Y. W., Hamilton, A., Arnuk, O. J., Chaftari, P., and Chemaly, R. Current drug therapy for multiple myeloma. Drugs, *57:* 485–506, 1999.
19. Joshua, D. E., MacCallum, S., and Gibson, J. Role of α interferon in multiple myeloma. Blood Rev., *11:* 191–200, 1997.
20. Shustik, C. Interferon in the treatment of multiple myeloma. Cancer Control, *5:* 226–234, 1998.
21. Powis, G., Mustacich, D., and Coon, A. The role of the redox protein thioredoxin in cell growth and cancer. Free Radic. Biol. Med., *29:* 312–322, 2000.
22. Dalton, W. S. Detection of multidrug resistance gene expression in multiple myeloma. Leukemia (Baltimore), *11:* 1166–1169, 1997.
23. Jonsson, B., Nilsson, K., Nygren, P., and Larsson, R. SDZ PSC-833: a novel potent *in vitro* chemosensitizer in multiple myeloma. Anticancer Drugs, *3:* 641–646, 1992.
24. Felts, S. J., Owen, B. A., Nguyen, P., Trepel, J., Donner, D. B., and Toft, D. O. The hsp90-related protein TRAP1 is a mitochondrial protein with distinct functional properties. J. Biol. Chem., *275:* 3305–3312, 2000.
25. Oda, E., Ohki, R., Murasawa, H., Nemoto, J., Shibue, T., Yamashita, T., Tokino, T., Taniguchi, T., and Tanaka, N. Noxa, a BH3-only member of the Bcl-2 family and candidate mediator of p53-induced apoptosis. Science (Wash. DC), *288:* 1053–1058, 2000.
26. Kickhoefer, V. A., Rajavel, K. S., Scheffer, G. L., Dalton, W. S., Scheper, R. J., and Rome, L. H. Vaults are up-regulated in multidrug-resistant cancer cell lines. J. Biol. Chem., *273:* 8971–8974, 1998.
27. Costantini, P., Colonna, R., and Bernardi, P. Induction of the mitochondrial permeability transition by *N*-ethylmaleimide depends on secondary oxidation of critical thiol groups. Potentiation by copper-ortho-phenanthroline without dimerization of the adenine nucleotide translocase. Biochim. Biophys. Acta, *1365:* 385–392, 1998.
28. Wang, T. S., Kuo, C. F., Jan, K. Y., and Huang, H. Arsenite induces apoptosis in Chinese hamster ovary cells by generation of reactive oxygen species. J. Cell. Physiol., *169:* 256–268, 1996.
29. Zhu, X. H., Shen, Y. L., Jing, Y. K., Cai, X., Jia, P. M., Huang, Y., Tang, W., Shi, G. Y., Sun, Y. P., Dai, J., Wang, Z. Y., Chen, S. J., Zhang, T. D., Waxman, S., Chen, Z., and Chen, G. Q. Apoptosis and growth inhibition in malignant lymphocytes after treatment with arsenic trioxide at clinically achievable concentrations. J. Natl. Cancer Inst., *91:* 772–778, 1999.
30. Zheng, J., Deng, Y. P., Lin, C., Fu, M., Xiao, P. G., and Wu, M. Arsenic trioxide induces apoptosis of HPV16 DNA-immortalized human cervical epithelial cells and selectively inhibits viral gene expression. Int. J. Cancer, *82:* 286–292, 1999.
31. Perkins, C., Kim, C. N., Fang, G., and Bhalla, K. N. Arsenic induces apoptosis of multidrug-resistant human myeloid leukemia cells that

express Bcr-Abl or overexpress MDR, MRP, Bcl-2, or Bcl-x_L. Blood, *95:* 1014–1022, 2000.

32. Ochi, T., Kaise, T., and Oya-Ohta, Y. Glutathione plays different roles in the induction of the cytotoxic effects of inorganic and organic arsenic compounds in cultured BALB/c 3T3 cells. Experientia (Basel), *50:* 115–120, 1994.
33. Akao, Y., Nakagawa, Y., and Akiyama, K. Arsenic trioxide induces apoptosis in neuroblastoma cell lines through the activation of caspase 3 *in vitro*. FEBS Lett., *455:* 59–62, 1999.
34. Larochette, N., Decaudin, D., Jacotot, E., Brenner, C., Marzo, I., Susin, S. A., Zamzami, N., Xie, Z., Reed, J., and Kroemer, G. Arsenite induces apoptosis via a direct effect on the mitochondrial permeability transition pore. Exp. Cell Res., *249:* 413–421, 1999.
35. Kroemer, G., and de The, H. Arsenic trioxide, a novel mitochondriotoxic anticancer agent? J. Natl. Cancer Inst. (Bethesda), *91:* 743–745, 1999.
36. Dai, J., Weinberg, R. S., Waxman, S., and Jing, Y. Malignant cells can be sensitized to undergo growth inhibition and apoptosis by arsenic trioxide through modulation of the glutathione redox system. Blood, *93:* 268–277, 1999.
37. Huang, S., Huang, C. F., and Lee, T. Induction of mitosis-mediated apoptosis by sodium arsenite in HeLa S3 cells. Biochem. Pharmacol., *60:* 771–780, 2000.
38. Ma, D. C., Sun, Y. H., Chang, K. Z., Ma, X. F., Huang, S. L., Bai, Y. H., Kang, J., Liu, Y. G., and Chu, J. J. Selective induction of apoptosis of NB4 cells from G_2+M phase by sodium arsenite at lower doses. Eur. J. Haematol., *61:* 27–35, 1998.
39. Li, Y. M., and Broome, J. D. Arsenic targets tubulins to induce apoptosis in myeloid leukemia cells. Cancer Res., *59:* 776–780, 1999.
40. Shen, Z. X., Chen, G. Q., Ni, J. H., Li, X. S., Xiong, S. M., Qiu, Q. Y., Zhu, J., Tang, W., Sun, G. L., Yang, K. Q., Chen, Y., Zhou, L., Fang, Z. W., Wang, Y. T., Ma, J., Zhang, P., Zhang, T. D., Chen, S. J., Chen, Z., and Wang, Z. Y. Use of arsenic trioxide (As_2O_3) in the treatment of acute promyelocytic leukemia (APL). II. Clinical efficacy and pharmacokinetics in relapsed patients. Blood, *89:* 3354–3360, 1997.
41. Soignet, S. L., Maslak, P., Wang, Z. G., Jhanwar, S., Calleja, E., Dardashti, L. J., Corso, D., DeBlasio, A., Gabrilove, J., Scheinberg, D. A., Pandolfi, P. P., and Warrell, R. P., Jr. Complete remission after treatment of acute promyelocytic leukemia with arsenic trioxide. N. Engl. J. Med., *339:* 1341–1348, 1998.
42. Rousselot, P., Labaume, S., Marolleau, J. P., Larghero, J., Noguera, M. H., Brouet, J. C., and Fermand, J. P. Arsenic trioxide and melarsoprol induce apoptosis in plasma cell lines and in plasma cells from myeloma patients. Cancer Res., *59:* 1041–1048, 1999.
43. Chen, G. Q., Shi, X. G., Tang, W., Xiong, S. M., Zhu, J., Cai, X., Han, Z. G., Ni, J. H., Shi, G. Y., Jia, P. M., Liu, M. M., He, K. L., Niu, C., Ma, J., Zhang, P., Zhang, T. D., Paul, P., Naoe, T., Kitamura, K., Miller, W., Waxman, S., Wang, Z. Y., de The, H., Chen, S. J., and Chen, Z. Use of arsenic trioxide (As_2O_3) in the treatment of acute promyelocytic leukemia (APL). I. As_2O_3 exerts dose-dependent dual effects on APL cells. Blood, *89:* 3345–3353, 1997.
44. Pestka, S. Identification of functional type I and type II interferon receptors. Hokkaido J. Med. Sci., *69:* 1301–1319, 1994.
45. Pestka, S. The human interferon-α species and hybrid proteins. Semin Oncol., *24:* S9-4–S9-17, 1997.
46. Voehringer, D. W. BCL-2 and glutathione: alterations in cellular redox state that regulate apoptosis sensitivity. Free Radic. Biol. Med., *27:* 945–950, 1999.
47. Powis, G., Kirkpatrick, D. L., Angulo, M., and Baker, A. Thioredoxin redox control of cell growth and death and the effects of inhibitors. Chem. Biol. Interact., *111–112:* 23–34, 1998.
48. Baker, A., Payne, C. M., Briehl, M. M., and Powis, G. Thioredoxin, a gene found overexpressed in human cancer, inhibits apoptosis *in vitro* and *in vivo*. Cancer Res., *57:* 5162–5167, 1997.
49. Powis, G., Briehl, M., and Oblong, J. Redox signalling and the control of cell growth and death. Pharmacol. Ther., *68:* 149–173, 1995.
50. Spyrou, G., Enmark, E., Miranda-Vizuete, A., and Gustafsson, J. Cloning and expression of a novel mammalian thioredoxin. J. Biol. Chem., *272:* 2936–2941, 1997.
51. Nomura, K., Imai, H., Koumura, T., Kobayashi, T., and Nakagawa, Y. Mitochondrial phospholipid hydroperoxide glutathione peroxidase inhibits the release of cytochrome *c* from mitochondria by suppressing the peroxidation of cardiolipin in hypoglycaemia-induced apoptosis. Biochem. J., *351:* 183–193, 2000.
52. Arch, R. H., and Thompson, C. B. Lymphocyte survival: the struggle against death. Annu. Rev. Cell Dev. Biol., *15:* 113–140, 1999.
53. Borg, A. G., Burgess, R., Green, L. M., Scheper, R. J., and Yin, J. A. Overexpression of lung-resistance protein and increased P-glycoprotein function in acute myeloid leukaemia cells predict a poor response to chemotherapy and reduced patient survival. Br. J. Haematol., *103:* 1083–1091, 1998.